Investigation of Microstructural Features, Phase Composition, and Magnetic Characteristics of YBCO-Based Composites and Additives of CuO Non-Superconducting Component Prepared in Low-Pressure Arc Discharge Plasma

I. V. Karpov[a, b, *], A. V. Ushakov[a, b], A. A. Lepeshev[a], V. G. Demin[b], L. Yu. Fedorov[a, b], E. A. Goncharova[b], G. M. Zeer[b], S. M. Zharkov[b, c], and A. K. Akbaryan[b]

[a] Federal Research Center, Krasnoyarsk Research Center, Siberian Branch, Russian Academy of Sciences, Krasnoyarsk, 660036 Russia
[b] Siberian Federal University, Krasnoyarsk, 660041 Russia
[c] Kirensky Institute of Physics, Subdivision of Federal Research Center, Krasnoyarsk Research Center, Siberian Branch, Russian Academy of Sciences, Krasnoyarsk, 660036 Russia
*e-mail: sfu-unesco@mail.ru

Abstract—A method making it possible to form HTS ceramics of non-superconducting coating consisting of self-organizing CuO crystals, whose sizes are less than the coherence length, i.e., within several tens of nanometers, has been developed. It has been shown that the combination of self-organizing structures in the form of whiskers and nanoparticles which arise as a result of combined sintering of $YBa_2Cu_3O_{(7-x)}$ powders and electric arc CuO nanopowders results in a significant increase in the current density and appearance of peak effect at high magnetic fields. Very high current density arises from the complex vortex pinning, where whisker defects provide high pinning energy and nanoparticles suppress flux creep. The morphology of such structures can be controlled by a simple change in the concentration of nanodisperse additives. It has been shown that 20 wt % of CuO additive is optimal.

Keywords: low-pressure arc discharge plasma, CuO nanopowder, pinning centers, high-temperature superconductor

INTRODUCTION

Critical current density J_c (and, accordingly, critical current I_c) is one of main characteristics of superconductors. The J_c value is very large at $H = 0$ in cuprate HTSs; however, it quickly decreases with an increase in H, which restricts the application of HTSs in high-power electrical devices and windings of powerful magnets at temperature of liquid nitrogen. To increase J_c, defects are added to superconductor, which represent pinning centers and prevent free displacement of magnetic vortices, which results in dissipation of energy. The problem is to determine optimal sizes and shape of pinning centers, as well as their number and arrangement in the specimen.

After ionic irradiation of single crystals of $YBa_2Cu_3O_{(7-x)}$, there is a significant increase in J_c, which indicates that radiation defects are the most effective pinning centers of magnetic flux [1]. Introduction of nanosized additives (NSAs) of inorganic materials to superconducting material is one of the promising methods for the formation of additional pinning centers and, consequently, an increase in

transport characteristics of HTSs [2, 3]. In this case, the choice of the impurities which are inert with respect to the superconducting matrix is necessary. Firstly, these impurities should not decrease the T_c value of the initial superconductor. Secondly, they would act as effective pinning centers upon addition to the superconducting material.

Effective pinning centers, which "anchor" eddies, are represented by the inclusions of impurity phases with the sizes corresponding to the length of superconducting coherence. Features of pinning in nanocomposite films of $YBa_2Cu_3O_{(7-x)}$ grown by chemical solution deposition and containing randomly oriented non-superconducting "nanodots" of $BaZrO_3$, Y_2O_3, $BaCeO_3$, and Ba_2YTaO_6 with the mean radius of 10–20 nm were studied in [4]. The record pinning force of greater than 20 GN/m^3 was achieved in the films containing about 10 mol % $BaZrO_3$.

The authors from [5] suggest a new pinning model according to which strain of the HTS matrix near nanodots results in the elongation of Cu—O bonds, as a result of which the pair suppression of holes at neigh-

boring copper nodes occurs and normal domains represented by pinning centers are formed.

Holesinger et al. [6] considered the mutual effect from columnar and planar defects grown by combined chemical solution deposition of organometallic compounds. These studies showed that the combined effect of random nanoparticles and columnar defects results in the increase in the critical current density at low and high fields. However, because microstructural defects depend strongly on the growth methods, it is not evident that this method could provide both random particles and columnar defects. It is important not only to control their growth and interaction but also to preserve constant composition.

B. Maiorov et al. [7] developed the procedure of $YBa_2Cu_3O_{(7-x)}$ film growth using pulsed laser deposition containing inclusions of the $BaZrO_3$ impurity phase of two types: randomly oriented nanoparticles and mainly uniaxially oriented (but at a small angle to each other) "columns." The concentration ratio of these defects can be controlled by varying the temperature of the substrate and the growth rate of the film upon its laser deposition, which is related to different kinetics of film growth. Combined analysis of the dependences of J_c on H and microstructure of films grown under various conditions showed that K_c is maximal in a strong field when the number of nanoparticles and "columns" is nearly identical. These results are explained by the authors from [7] by the creep suppression of magnetic flux, which is caused by the expansion of a double kink on the vortex, which is bound simultaneously to two "columns." They suggest that the absence of nanoparticles in single crystals, which are much more effective pinning centers than point radiation defects, which are formed upon irradiation with the "columns," is the reason for the lower J_c value of single crystals.

The aim of this work is to study the effect of the concentration of non-superconducting nanosized CuO additives on the superconducting characteristics of $YBa_2Cu_3O_{(7-x)}$ + nano CuO polycrystalline composites at the temperature of liquid nitrogen.

EXPERIMENTAL

The powder of $YBa_2Cu_3O_{(7-x)}$ precursor was prepared through solid-phase synthesis. The $YBa_2Cu_3O_{(7-x)}$/nano-CuO composite was modified using a device described in detail in [8]. Copper of M00b brand was chosen as the cathode for sputtering. The HTS powder was first exposed to purification in a glow discharge at the voltage of 1000 V on the substrate for 1 min; activation by ionic bombardment was carried out for 1 min at the arc discharge current of 20 A and the voltage of 1000 V on the substrate. The rotation frequency of the mixing unit was 8 min^{-1}, the vibration amplitude was 1 mm, and vibration frequency was 50 Hz. Direct deposition of copper oxide nanoparticles onto HTS micrograins was carried out at the discharge current of

500 A and the longitudinal magnetic field intensity generated by the focusing coil was 80 Oe on the cathode surface. To carry out plasma chemical reactions, a 10% O_2 + 90% Ar gas mixture was charged to the chamber after preliminary vacuum pumping to the pressure of 10^{-3} Pa using a two-channel gas flow regulator. Synthesis was carried under the pressure starting from 60 Pa. After deposition of nanoparticles, the specimens were passivated in an atmosphere of pure oxygen for one day. The weight concentrations of the additives were 0.5, 5, 15, and 20%.

The obtained mixture was pressed into pellets 10 mm in diameter and 1 mm in height under the pressure of 10 MPa. Then, the grains were sintered at 940°C for 24 h with subsequent exposure at 400°C and final cooling to room temperature in the furnace in the air.

Structural studies of the specimens were carried out on a JEOL JSM-7001F scanning electron microscope.

Magnetic measurements were carried out using an MPMS-XL5 unit. X-ray diffraction patterns were recorded on a D8 ADVANCE diffractometer (Bruker AXS). The isothermal dependences of magnetization on the magnetic field were measured at the temperature of 4–77 K. The critical current density of the specimens was evaluated according to the magnetic hysteresis loop using the model of expanded critical state.

RESULTS AND DISCUSSION

Figure 1 shows the diffraction patterns of the YBCO + xCuO composites (x = 0.5, 5, 15, and 20 wt %) at room temperature. Analysis of the diffraction pattern showed that all specimens crystallize in the orthorhombic phase with the *Pmmm* space group. The lattice parameters and other determined parameters of all specimens are given in Table 1.

The presence of CuO peaks in the YBCO matrix is illustrated by additional peaks in the diffraction pattern, whose intensity increases with an increase in the concentration of CuO in YBCO. The monoclinic (2θ = 35.44, 35.56, 38.78, and 48.76; *hkl*: (002), (−111), (111), and (−202)) phase of CuO nanoparticles was detected. Full-profile analysis of the diffractograms according to the Ritveld method showed that plasma treatment of HTS and addition of more than 5 wt % of copper oxide result in the formation of two orthorhombic phases with different lattice parameters. The effect of the concentration of copper oxide nanopowder on the magnitude of residual stresses of the YBCO + xCuO composites was investigated. The results are given in Table 1. Change in the phase composition of the composite should significantly affect their magnetic and transport characteristics. Figure 2 shows the SEM micrograph of the YBCO + xCuO composite. The nanopowder is homogeneously distributed along the surface of YBCO particles and also fills the intergranular space and pores, which can act as a catalyst to improve the structural quality at grain boundaries. This forces the grain to act consistently and significantly changes the
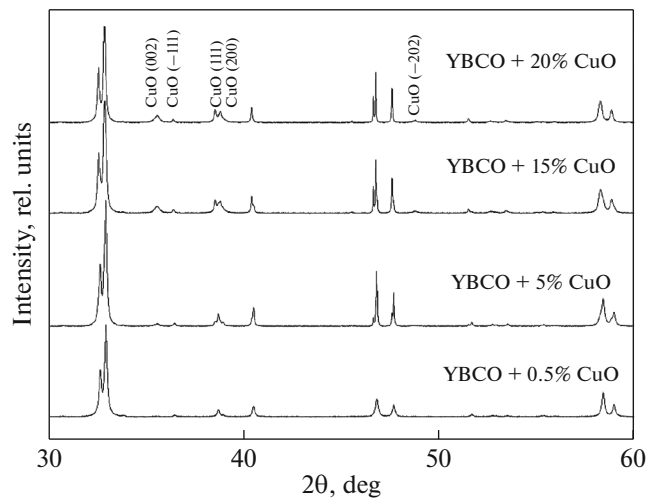
Fig. 1. X-ray diffraction patterns of the YBCO + xCuO composites (x = 0.5, 5, 15, and 20 wt %).

Fig. 2. SEM micrographs of the YBCO + xCuO composites (x = (a) 15 and (b) 20 wt %).

mechanical and transport measurements. It should be noted that self-organized structures in the form of whiskers arise along with agglomerates at the concentration of copper oxide nanopowder of 20 wt %.

Figure 3 shows the results of the magnetization study of the specimens. As follows from the results of the studies, the behavior of hysteresis curves agrees well with the results of the study of phase composition and microstructure. The appearance of two orthorhombic phases in the composites with the additives of 5 and 15 wt % CuO results in the shift of H_{C1} to higher values and, consequently, a decrease in critical current, in particular, at high fields. Addition of 20 wt % CuO results in a remarkable (more than threefold) increase in the peak value of magnetization both at Meissner currents and at high fields. To study this effect in detail, the magnetic properties were investigated at high temperatures.

Critical current densities J_c for YBCO-doped superconductors at 77 K depending on magnetic field B are given in Fig. 4 at the concentration xCuO = 10 and 20 wt %, respectively.

The corresponding dependences of critical temperatures T_c and transition band width ΔT_c on the concentration x of CuO are given in Fig. 5 and Table 2.

The specimens of the YBCO + CuO composites with 10 wt % of nano-CuO demonstrate a slight increase in the current density J_c at magnetic field B in the range from 0 to 1 T, which indicates enhancement of magnetic flux pinning due to non-superconducting inclusions. They result in the lattice distortions at the interface and affect the distribution of oxygen-deficient domains with low J_c. However, the subsequent increase in magnetic field results in a nearly stepwise decrease in current density to 0. In this range of magnetic fields, dissipation is intrinsic to the magnetic flux creep model with the temperature-independent pinning energy $U(H)$. As follows from Fig. 5, addition
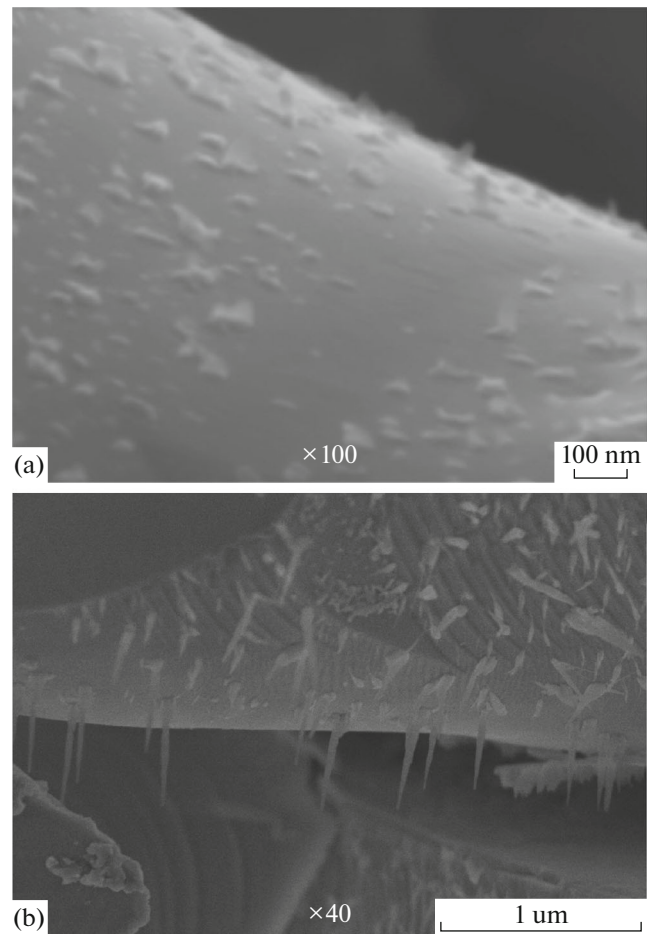
of 10 wt % of nanodispersed CuO powder results in a decrease in critical temperature T_c and an increase in the transition band width, which confirms the statements above.

Figure 6 gives the dependences of critical current densities J_c on magnetic field B for the YBCO + CuO composites with 10 and 20 wt % CuO at 70 K. The

Table 1. Lattice parameters of YBCO in the composite

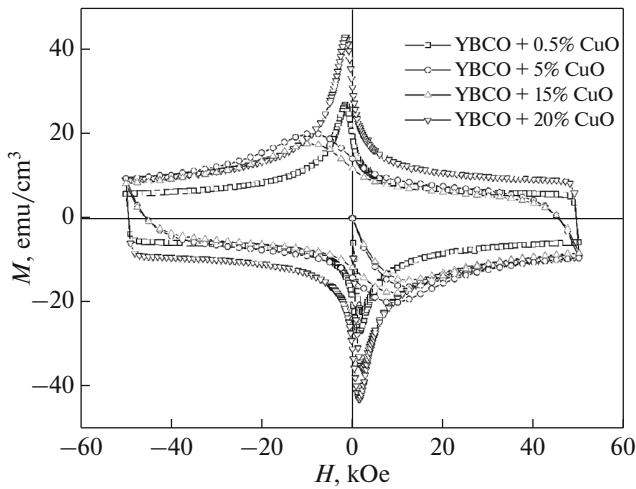| Specimen	a(Å)	b(Å)	c(Å)	Residual stresses, MPa
YBCO	3.825	3.888	11.695	—
YBCO + 0,5% CuO	3.826	3.893	11.681	45
64,9%YBCO1 + 5%CuO + 34,6%YBCO2	3.828 / 3.884	3.890 / 3.8193	11.688 / 11.681	50
44,8%YBCO1 + 15%CuO + 50,2%YBCO2	3.828 / 3.881	3.890 / 3.8189	11.688 / 11.687	67
YBCO2 + 20%CuO	3.879	3.8185	11.679	73

Fig. 3. Isothermal magnetization hysteresis loops of the YBCO + xCuO composites (x = 0.5, 5, 15, and 20 wt %) at 5 K.
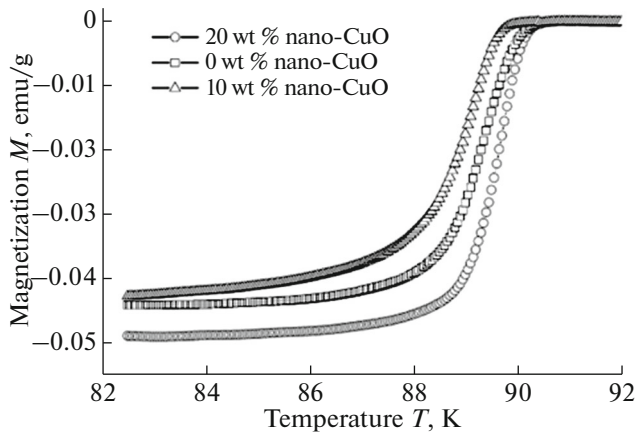

Fig. 4. Dependence of critical current density values J_c on magnetic field B of the YBCO + xCuO composites, with x = 10 and 20 wt % at 77 K.

Fig. 5. Dependences of magnetization on temperature for various concentrations of nano-CuO in the composites.

Fig. 6. Dependence of critical current density values J_c on magnetic field B of the YBCO + xCuO composites, with x = 10 and 20 wt % at 70 K.

critical current density J_c of the specimens significantly increases at the magnetic field B of 0 to 1 T; however, the form of the curve remains on the whole typical, as in the case of 77 K. The composite specimens YBa$_2$Cu$_3$O$_{(7-x)}$–CuO with 20 wt % nano-CuO demonstrate a significant increase in the critical current density J_c in the entire range of the applied magnetic field B (Fig. 4). In addition, the specimens display a clear peak effect in the magnetic field B from 1 to 2 T. If the plots for the YBCO + CuO with 20 wt % CuO are compared (Fig. 4), it becomes evident that the magnetic flux pinning is enhanced in the magnetic field B range from 0 to 1 T owing to non-superconducting inclusions of drop-shaped CuO.

However, an increase in the critical current density J_c and, in particular, peak effect are presumably caused by the appearance of non-superconducting
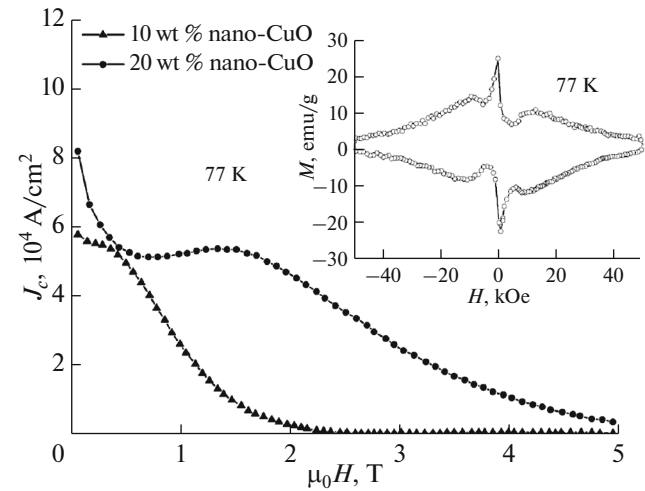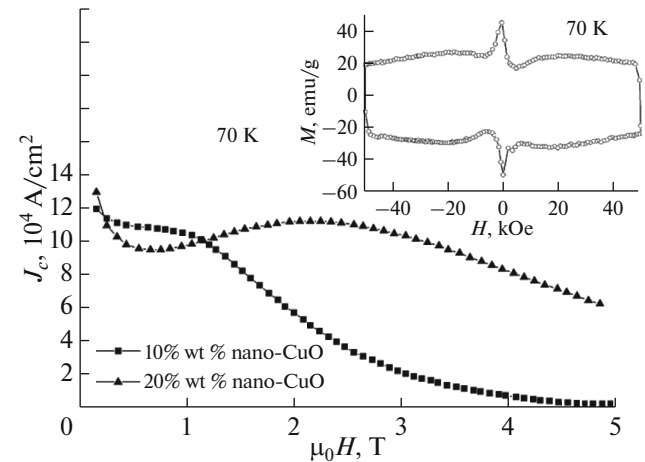
inclusions of CuO in the form of whickers at magnetic field B from 1 to 5 T of the YBCO + CuO composites with 20 wt % CuO. In such composites, a complex interaction of two types of defects represented by drops and whiskers is intrinsic. Thus, the whisker defects give the main contribution to the pinning force, while "auxiliary" pinning on drops prevents creep. Figure 6 is a clear illustration of this concept. In addition to a significant increase in the critical current density J_c of the YBCO + 20 wt % CuO composite, the peak effect displays a temperature dependence. The peak value B_p corresponds to 1.5 and 2.5 T at 77 and 70 K. As follows from Fig. 4, the whisker defects affect the critical temperature T_c and the transition band width ΔT_c. These values are 91 and 0.5 K in the YBCO + 20 wt % CuO. Strain models of the increase in the transition temperature in bulk superconductor (T_c)

Table 2. Critical temperatures T_c and the transition band width ΔT_c in the YBCO + CuO composites

Specimen	T_c, K	ΔT_c, K
YBCO	89.5	0.85
YBCO + 10% CuO	88.5	1.0
YBCO + 20% CuO	91.0	0.5

due to the lattice defects are given in [9]. It was shown in [10] that the bulk values of T_c depend strongly on pressure, which arises owing to local strains of nanoparticles, with anisotropy. This effect is explained by the increase in the coherence length. It is shown in Table 1 that strains around the array of dislocations, which are related to whisker defects, can be significant. An increase in T_c can be evaluated on intercrystallite boundaries determining the superconducting state, edge dislocations [11, 12], small-angle grain boundaries, and metastable linear dislocation arrays. Changes in the YBCO + 20 wt % CuO composites, which are related to the strains from defects, and an increase in T_c affect magnetic flux pinning.

CONCLUSIONS

Thus, addition of up to 20 wt % of non-superconducting nanosized CuO powders prepared in the low-pressure arc discharge plasma to polycrystalline $YBa_2Cu_3O_{(7-x)}$ HTSs results in the design of novel type of composites with nanosized defects in the form of drops and whiskers. Study of superconducting characteristics of the composites has revealed a remarkable increase in the critical current density and peak effect at strong magnetic fields. The main contribution to the pinning force is given by the whisker defects, while "auxiliary" pinning on drops prevents creep. The whisker defects are responsible for an increase in the critical temperature T_c and a decrease in the transition band width ΔT_c.

FUNDING

REFERENCES

1. Podlivaev, A.I., Pokrovskii, S.V., Anischenko, I.V., and Rudnev, I.A., Precise magnetometric diagnostics of critical-current inhomogeneities in high-temperature semiconductor tapes, *Tech. Phys. Lett.*, 2017, vol. 43, no. 12, pp. 1136−1139.

2. Ushakov, A.V., Karpov, I.V., Lepeshev, A.A., Petrov, M.I., Fedorov, L.Yu., Gokhfel'd, D.M., Zharkov, S.M., Zeer, G.M., Demin, V.G., and Abkaryan, A.K., The influence of CuO dopant nanoparticles, prepared via the arc plasma synthesis method, on the critical current of $YBa_2Cu_3O_{7-\sigma}$ composites, *Inorg. Mater.: Appl. Res.*, 2019, vol. 10, no. 4, pp. 999−1002.
https://doi.org/10.1134/S2075113319040439

3. Ushakov, A.V., Karpov, I.V., Fedorov, L.Yu., Dorozhkina, E.A., Karpova, O.N., Shaikhadinov, A.A., Demin, V.G., Demchenko, A.I., Brungardt, M.V., and Goncharova, E.A., Formation of CuO and Cu_2O crystalline phases in a reactor for low-pressure arc discharge synthesis, *Inorg. Mater.: Appl. Res.*, 2020, vol. 11, no. 1, pp. 232−237.
https://doi.org/10.1134/S2075113320010372

4. MacManus-Driscoll, J.L., Foltyn, S.R., Jia, Q.X., Wang, H., Serquis, A., Civale, L., Maiorov, B., Hawley, M.E., Maley, M.P., and Peterson, D.E., Strongly enhanced current densities in superconducting coated conductors of $YBa_2Cu_3O_{7-x}$ + $BaZrO_3$, *Nat. Mater.*, 2004, vol. 3, no. 4, pp. 439−443.

5. Llordés, A., Palau, A., Gázquez, J., Coll, M., Vlad R., Pomar, A., Arbiol, J., Guzmán, R., Ye, S., Rouco, V., Sandiumenge, F., Ricart, S., Puig, T., Varela, M., Chateigner D., et al., Nanoscale strain-induced pair suppression as a vortex-pinning mechanism in high-temperature superconductors, *Nat. Mater.*, 2012, vol. 11, no. 4, pp. 329−336.

6. Holesinger, T.G., Civale, L., Maiorov, B., Feldmann, D.M., Coulter, J.Y., Miller, D.J., Maroni, V.A., Chen, Z., Larbalestier, D.C., Feenstra, R., Li, X., Huang, Y., Kodenkandath, T., Zhang, W., Rupich, M.W., et al., Progress in nanoengineered microstructures for tunable high-current, high-temperature superconducting wires, *Adv. Mater. Prog. Rep.*, 2008, vol. 20, pp. 391−407.

7. Maiorov, B., Baily, S.A., Zhou, H., Ugurlu, O., Kennison, J.A., Dowden, P.C., Holesinger, T.G., Foltyn, S.R., and Civale, L., Synergetic combination of different types of defect to optimize pinning landscape using $BaZrO_3$−doped $YBa_2Cu_3O_7$, *Nat. Mater.*, 2009, vol. 8, pp. 398−404.

8. Karpov, I.V., Ushakov, A.V., Lepeshev, A.A., Fedorov, L.Yu., Dorozhkina, E.A., Karpova, O.N., Shaikhadinov, A.A., and Demin, V.G., Device for increasing the magnetic flux pinning in granular nanocomposites based on the high-temperature superconducting ceramic, *Tech. Phys.*, 2018, vol. 63, no. 2, pp. 230−234.
https://doi.org/10.1134/S1063784218020196

9. Miura, S., Ichino, Y., Yoshida, Y., Ichinose, A., and Tsuruta, A., Vortex pinning properties at grain boundary in $SmBa_2Cu_3O_y$ superconducting films with $BaHfO_3$ nanorods controlled via low-temperature growth, *IEEE Trans. Appl. Supercond.*, 2017, vol. 27, no. 4, p. 7781616.

10. Gasumyants, V.E. and Martynova, O.A., Experimental investigation and quantitative analysis of the normal-state Nernst coefficient in doped high-temperature superconductors of the $YBa_2Cu_3O_y$ system, in *High-Temperature Superconductors: Occurrence, Synthesis and Applications*, Miryala, M. and Koblischka, M.R., Eds., New York: Nova Science, 2018, chap. 5, pp. 92−152.

11. Salafranca, J., Rincon, J., Tornos, J., Leon, C., Santamaria, J., Dagotto, E., Pennycook, S.J., and Varela, M., Competition between covalent bonding and charge transfer at complex-oxide interfaces, *Phys. Rev. Lett.*, 2014, vol. 112, no. 19, p. 196802.

12. Patala, S. and Schuh, C.A., Symmetries in the representation of grain boundary-plane distributions, *Philos. Mag.*, 2013, vol. 93, no. 5, pp. 524−573.

Translated by A. Muravev